EUROPHYSICS LETTERS 15 July 2004

Europhys. Lett., **67** (2), pp. 198–204 (2004)
DOI: 10.1209/epl/i2004-10059-y

Buffer gas cooling and trapping of atoms with small effective magnetic moments

J. G. E. Harris[1,2], R. A. Michniak[1,2], S. V. Nguyen[1,2], N. Brahms[1,2], W. Ketterle[1,3] and J. M. Doyle[1,2]

[1] *Harvard/MIT Center for Ultracold Atoms - Cambridge, MA 02138, USA*
[2] *Department of Physics, Harvard University - Cambridge, MA 02138, USA*
[3] *Department of Physics, MIT - Cambridge, MA 02139, USA*

(received 5 April 2004; accepted 10 May 2004)

PACS. 32.80.Pj – Optical cooling of atoms; trapping.
PACS. 39.25.+k – Atom manipulation (scanning probe microscopy, laser cooling, etc.).
PACS. 68.43.Mn – Adsorption/desorption kinetics.

Abstract. – We have extended buffer gas cooling to trap atoms with small effective magnetic moments $\mu_{\rm eff}$. For $\mu_{\rm eff} \geq 3\mu_{\rm B}$, 10^{12} atoms were buffer gas cooled, trapped, and thermally isolated in ultra high vacuum with roughly unit efficiency. For $\mu_{\rm eff} < 3\mu_{\rm B}$, the fraction of atoms remaining after full thermal isolation was limited by two processes: wind from the rapid removal of the buffer gas and desorbing helium films. In our current apparatus we trap atoms with $\mu_{\rm eff} \geq 1\mu_{\rm B}$, and thermally isolate atoms with $\mu_{\rm eff} \geq 1.8\mu_{\rm B}$. This triples the number of atomic species which can be buffer gas cooled and trapped in thermal isolation. Extrapolation of our results and simulations of the loss processes indicate that it is possible to trap and evaporatively cool $1\mu_{\rm B}$ atoms using buffer gas cooling.

Buffer gas cooling is a powerful tool for producing cold atoms [1]. It relies only upon elastic collisions with a cryogenic helium vapor for cooling, and so is applicable to any atomic species. This is crucial because other methods of cooling (*e.g.*, laser cooling [2] or cooling via superfluid walls [3]) are applicable to only a limited range of species, nearly all of which are S-state atoms whose interactions are dominated by spherically symmetric, short-range potentials (the one exception is Cr, for which magnetic dipolar interactions play a significant role [4]). The production of cold, non-S-state atoms and atoms with a variety of magnetic dipole moments would allow the study of new regimes of atomic collisions [5]. Because many of the properties of a degenerate gas are determined by the collisional properties of its constituents, Bose-condensing these atoms has been predicted to result in qualitatively new types of quantum fluids [6].

The wide applicability of buffer gas cooling also means that it can be used to create cold samples of atoms which are of interest for high-precision spectroscopy but which cannot be laser cooled [7]. It is also capable of cooling arbitrary mixtures of different species and isotopes. Lastly, buffer gas cooling combines these advantages with the ability to produce orders-of-magnitude larger samples of cold atoms than laser cooling. Regardless of the atomic species, larger samples provide improved sensitivity (*e.g.*, for atom interferometers and precision spectroscopy), and lead to new regimes of hydrodynamic quantum gases [8].

A shortcoming of buffer gas cooling is that the cooled atoms are initially embedded in the He buffer gas. Many of the goals mentioned above require cold atoms trapped in thermal isolation (*i.e.*, good vacuum), both to allow further cooling by evaporation and to eliminate collisions with the He. Previously, buffer gas cooled atoms were magnetically trapped and the buffer gas was removed by using a dilution refrigerator to cool the cell walls below 200 mK, cryopumping the He [9]. This method of buffer gas pumping was limited to atoms with large magnetic moments μ, as only these atoms had trap lifetimes long enough to survive the several seconds required to pump out the He. More than 10^{12} atoms with $\mu \geq 6\mu_{\mathrm{B}}$ were trapped in excellent vacuum this way [9, 10], but the long time required to remove the buffer gas prevented the trapping of a wider range of atoms.

Here we demonstrate a new technique that dramatically increases the range of atomic species which can be buffer gas cooled and magnetically trapped in good vacuum. The key innovation is an entirely new approach to buffer gas management which achieves vacuum more than two orders of magnitude faster than was previously possible. This allows us to trap and thermally isolate large numbers of atoms with magnetic moments of $1.8\mu_{\mathrm{B}}$ or greater. This triples the number of species that can be buffer gas cooled, trapped and thermally isolated, and bridges the gap between atoms which can be buffer gas cooled and those which have been Bose condensed (all of which have $\mu \leq 2\mu_{\mathrm{B}}$). Our experiments show that there are no fundamental impediments to extending this technique to $1\mu_{\mathrm{B}}$ atoms, opening the way to a number of the goals described above.

The essential requirement for buffer gas trapping is that the buffer gas be removed on a time scale shorter than the trap lifetime of the atoms in the buffer gas. Numerical simulations [11] (and the experiments described here) show that collisions with the buffer gas limit the trap lifetime to ~ 40 ms for $\mu = 1\mu_{\mathrm{B}}$, increasing to ~ 20 s for $6\mu_{\mathrm{B}}$ atoms. This assumes a trap depth $B_{\mathrm{trap}} = 4$ T [12] and He temperature $T_{\mathrm{He}} = 500$ mK (T_{He} must be high enough to ensure adequate He density n_{He} to cool the atoms). In this work, we use a rapidly actuating, high-conductance cryogenic valve and *in situ* cryopump to quickly achieve vacuum adequate for evaporative cooling. This allows us to forego the expense and complexity of a dilution refrigerator.

Three obstacles make it difficult to rapidly achieve good vacuum in a buffer gas cell: limited pumping speed for the ^{3}He buffer gas, virtual leaks (*e.g.* from fill lines), and desorption of ^{3}He from cell walls. The first two issues are directly addressed in the design of our cell (fig. 1). A pneumatically actuated, large-aperture cryogenic valve connects the trapping region to a pumping region with ~ 30 g of activated charcoal cooled to 1.5 K by the ^{4}He pot of a ^{3}He refrigerator. The estimated conductance of this valve and the volume of the cell ($V = 0.5$ l) give a pumpout time $\tau_{\mathrm{pump}} = 50$ ms (100 ms) for ^{3}He gas at 500 mK in the viscous (molecular) regime [13].

τ_{pump} would be substantially increased if the buffer gas also had to be removed from narrow fill lines connecting the cell to the room temperature gas handling system. This is avoided by introducing the ^{3}He into the trapping region through a high-impedance orifice (2×10^{-4} l/s) from an "antechamber" (fig. 1) containing a small sorb. Once the trapping region is filled with ^{3}He, we evacuate both the antechamber and its fill line by cooling this sorb below 2 K. Then we produce the atoms (via laser ablation of a solid target [14]) and after some delay open the valve (which actuates 2 cm in 20 ms), pumping the ^{3}He gas onto the large sorb and leaving the magnetic atoms in the trap.

Because the trap lifetime depends upon μ only via the product μB_{trap}, we simulate atoms of different effective magnetic moment μ_{eff} by using Cr ($\mu = 6\mu_{\mathrm{B}}$) and varying B_{trap} (*i.e.*, $\mu_{\mathrm{eff}} = \mu B_{\mathrm{trap}}/B_{\mathrm{trap}}^{\mathrm{max}}$, where $B_{\mathrm{trap}}^{\mathrm{max}} = 3.9$ T is the deepest trap achievable with our magnet [12]). Other aspects of the buffer gas cooling process such as the introduction of atoms into the buffer

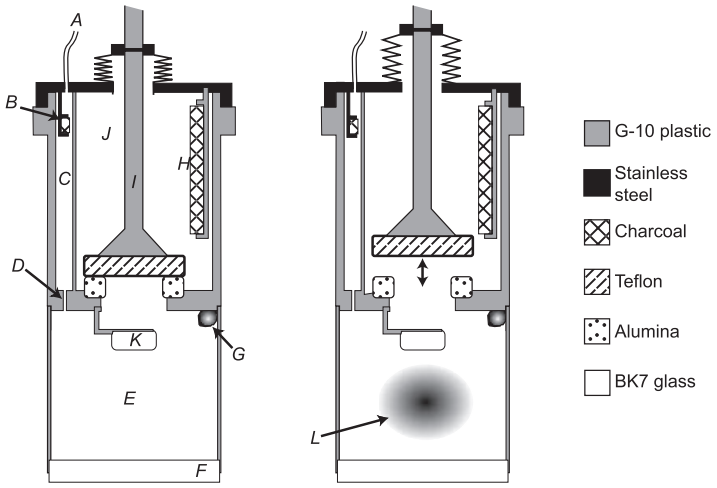

Fig. 1 – Schematic cross-section of the buffer gas cell with the valve closed (left) and open (right). *A*: fill line; *B*: small sorb; *C*: antechamber; *D*: high-impedance orifice; *E*: trapping region; *F*: window; *G*: Cr ablation target; *H*: large sorb; *I*: valve shaft; *J*: pumping region; *K*: mirror; *L*: trapped atoms.

gas cell and their thermalization with the helium vapor have previously been demonstrated using a wide range of atoms and molecules [9, 10, 14–16]. The atoms are probed via the absorption of a laser beam tuned to the $^7S_3$-$^7P_4$ transition of Cr (425 nm).

Figure 2(a) shows the time dependence of the peak density of Cr atoms $n_{\rm Cr}(t)$ in the trap for $\mu_{\rm eff} = 3\mu_{\rm B}$. Similar behavior is seen for larger $\mu_{\rm eff}$. Initially, the cell is filled to $n_{\rm He} = 6.2 \times 10^{15}\,{\rm cm}^{-3}$ [17]. The ablation laser fires at $t = 0\,{\rm s}$, producing hot Cr atoms, $N_{\rm Cr} = 5.5 \times 10^{11}$ of which thermalize in the maximally trapped $m_J = 3$ state (m_J is the magnetic quantum number) at a temperature $T_{\rm Cr} = 600\,{\rm mK}$ and density $n_{\rm Cr} = 1.2 \times 10^{12}\,{\rm cm}^{-3}$. $T_{\rm Cr}$, $N_{\rm Cr}$ and $n_{\rm Cr}$ are determined by fitting the trapped atoms' Zeeman-broadened absorption spectrum to that of a Boltzmann distribution of atoms in our magnetic trap, as described in refs. [10, 14]. The inset of fig. 2(a) shows one such spectrum and fit.

After the ablation and before the valve opens ($0\,{\rm s} < t < 2.5\,{\rm s}$ in fig. 2(a)), the Cr atoms are confined by the trap and move diffusively in the ^{3}He. Cr is lost from the trap via both dipolar relaxation and evaporation, and $T_{\rm Cr}$ tracks $T_{\rm cell}$, the cell temperature (shown in the inset of fig. 3(a)), indicating the trapped Cr is still in thermal contact with the cell walls. At $t = 2.5\,{\rm s}$, the valve opens, the ^{3}He rushes out of the cell to the large sorb and the trapped Cr is left behind. A small fraction, $x_{\rm wind}$, of the Cr atoms (too small to be visible in fig. 2(a)) is carried out of the trap with the ^{3}He "wind". As one would expect, and in good qualitative agreement with numerical simulations [11], $x_{\rm wind}$ increases for increasing $n_{\rm He}$ and decreasing $B_{\rm trap}$. This "wind loss" occurs in the $\sim 200\,{\rm ms}$ immediately after the valve is opened, while most of the ^{3}He flows out of the cell.

After the ^{3}He is removed, $T_{\rm Cr}$ remains constant (600 mK) and $n_{\rm Cr}$ gradually decreases due to 2-body collisions. This can be seen from the fit in fig. 2(a) of the form $n_{\rm Cr}(t) = n_0/(1 + n_0\Gamma_2\,t/8)$. The two fitting parameters are $n_0 = n_{\rm Cr}(0)$ and Γ_2, the two-body rate coefficient. The value of Γ_2 agrees well with previous measurements [10]. The trap loss is due to dipolar relaxation to untrapped m_J states and causes heating of the cloud. Cooling via evaporation over the top of the trap balances this heating and leads to an equilibrium in which $\eta = \mu B_{\rm trap}/k_{\rm B}T_{\rm Cr}$ is independent of time [18].

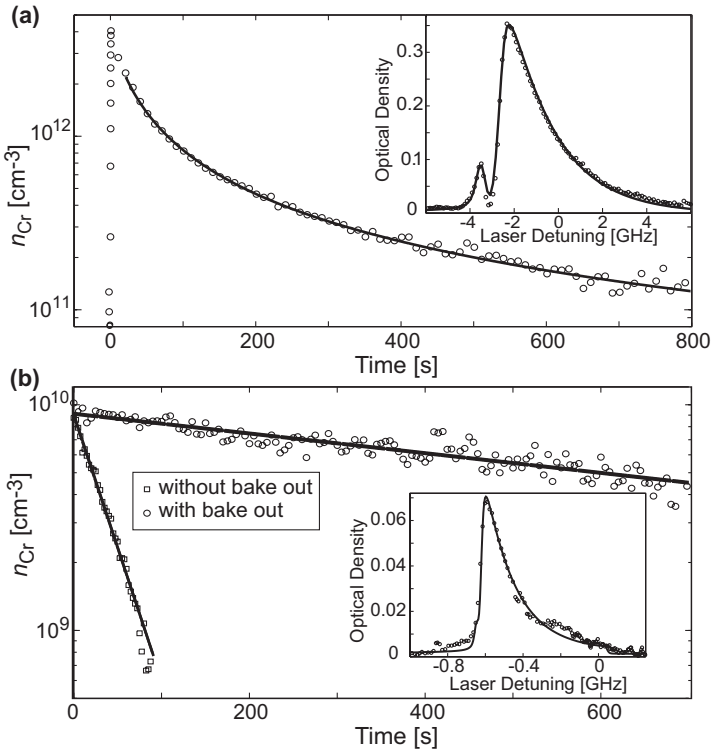

Fig. 2 – Trapping and evaporative cooling of atoms with $3\mu_B$ effective magnetic moment. (a) Decay of the peak density of trapped Cr. Solid line: fit to two-body loss. Inset: spectrum of trapped Cr 5 s after the valve opens. The fit gives $T_{Cr} = 600\,\text{mK}$, $n_{Cr} = 1.2 \times 10^{12}\,\text{cm}^{-3}$ and $N_{Cr} = 5.5 \times 10^{11}$ atoms. (b) $n_{Cr}(t)$ after evaporative cooling. The bake-out data has been scaled to match the no-bake-out data at $t = 0$. The lines are fits to exponential decay and show that baking the cell increases the trap lifetime from 37 s to 995 s. Inset: spectrum of trapped Cr atoms after evaporative cooling. The fit gives $T_{Cr} = 47\,\text{mK}$, $n_{Cr} = 3.6 \times 10^9\,\text{cm}^{-3}$ and $N_{Cr} = 9.8 \times 10^{10}$ atoms. Only the peak at $-0.6\,\text{GHz}$ (due to ^{52}Cr) is fit. The shoulder at $-0.2\,\text{GHz}$ is due to ^{53}Cr.

In order to show that the trapped Cr atoms are thermally isolated from the cell walls, we lower T_{Cr} by decreasing B_{trap} (cooling occurs via evaporation and adiabatic expansion), as shown in fig. 2(b). Here 10^{12} Cr atoms were trapped as described above, and after opening the valve B_{trap} was reduced by a factor of 50 to 39 mT. The inset of fig. 2(b) shows a spectrum taken after this cooling with a fit giving $T_{Cr} = 47\,\text{mK}$. The decay of n_{Cr} (squares in fig. 2(b)) is exponential and hence no longer dominated by two-body processes, but rather by one-body. Fitting this data to $n_{Cr}(t) = n_{Cr}(0)e^{-t/\tau_1}$ gives a one-body time constant $\tau_1 = 37\,\text{s}$. One-body loss is absent in fig. 2(a) because there $B_{trap} = 1.95\,\text{T}$ and so the Cr atoms see a trap substantially deeper than the mean thermal energy of a background gas atom $k_B T_{cell}$. For $T_{cell} = 500\,\text{mK}$, only one Cr-^{3}He collision in 10^{28} ejects a Cr atom from the trap. However for $B_{trap} = 39\,\text{mT}$, this ratio is roughly unity and τ_1 provides a direct measure of the background gas density $n_{He} = (\tau_1 \sigma \nu)^{-1} = 4.5 \times 10^8\,\text{cm}^{-3}$, where $\sigma = 10^{-14}\,\text{cm}^2$ is the Cr-^{3}He elastic cross-section [14] and $\nu = 5300\,\text{cm/s}$ is the mean thermal velocity of the ^{3}He. This level of background gas does not impede the evaporative cooling (note that $\tau_1 = 30\,\text{s}$ or even 5 s is adequate to achieve BEC in other experiments [18, 19]).

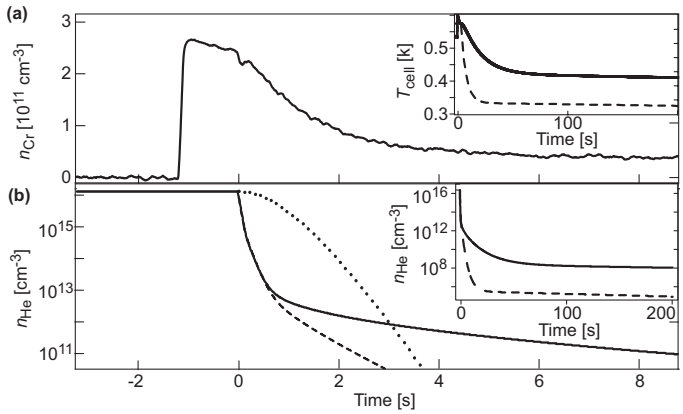

Fig. 3 – Trap loss due to the ^{3}He film. (a) Decay of the peak density of trapped Cr for $\mu_{\rm eff} = 2.45\mu_{\rm B}$. The inset shows the cell temperature. Solid line: measured $T_{\rm cell}$. The initial rise is due to the ablation. The cell cools to 420 mK after the valve opens. Dashed line: $T_{\rm cell}$ calculated for a base temperature of 320 mK and a cooling rate four times that of the present cell. (b) Solid line: ^{3}He density in the cell as a function of time, calculated using the model described in the text and the measured $T_{\rm cell}(t)$. Dashed line: $n_{\rm He}(t)$ calculated for an improved $T_{\rm cell}(t)$ (dashed line in inset of (a)). Dotted line: $n_{\rm He}(t)$ calculated for the experiments of ref. [10], in which the buffer gas was removed by lowering $T_{\rm cell}$. Inset: the same calculations for longer times.

The fact that $n_{\rm He}$ remains roughly constant after reaching $4.5 \times 10^8\,{\rm cm}^{-3}$ implies a flux of 2.3×10^{12} ^{3}He atoms/s into the cell volume. This flux is due to desorption of the thin ^{3}He film which coats the cell each time it is filled with buffer gas. We demonstrate that this film is responsible for the 37 s lifetime described above by "baking out" the cell (in analogy with the bake-out of water films in room temperature UHV systems). After filling the cell with buffer gas, ablating, trapping 10^{12} Cr atoms, and removing the buffer gas all with $B_{\rm trap} = 1.95$ T, we heat the cell from 520 mK to 650 mK for 60 s. We then allow the cell to cool back to 470 mK. Only then do we evaporatively cool the Cr atoms by decreasing $B_{\rm trap}$ to 39 mT. By following this procedure, we find that τ_1 is increased to $\sim 10^3$ s (circles in fig. 2(b)).

The behavior of the trapped atoms depends strongly upon $\mu_{\rm eff}$. For $\mu_{\rm eff} < 3\mu_{\rm B}$, we observe enhanced atom loss in the first seconds after the valve opens. Figure 3(a) shows $n_{\rm Cr}(t)$ for $\mu_{\rm eff} = 2.45\mu_{\rm B}$. Ablation occurs at $t = -1.2$ s and the valve opens at $t = 0$ s. There is $\sim 75\%$ atom loss in the first 5 s after the valve opens. After this $n_{\rm Cr}$ remains nearly constant, decaying only very slowly via Cr-Cr collisions as in fig. 2(a). The loss seen in fig. 3(a) cannot be attributed to the ^{3}He wind, which occurs only in the first 200 ms after the valve opens. Instead, this loss is due to collisions of Cr with ^{3}He atoms desorbing from the cell wall.

We model this desorption using simple gas dynamics: the ^{3}He desorption rate [13] $\dot{n}_{\rm d} = P(d) f A/V \sqrt{2\pi k_{\rm B} T_{\rm cell}(t) m}$, where m is the ^{3}He mass, f is the sticking fraction (taken to be 0.75) [20], $A = 420\,{\rm cm}^2$ is the surface area of the cell, and the vapor pressure P is related to the film thickness d and the saturated vapor pressure P_0 by the FHH expression [21] $P = P_0 \exp[-\alpha/T_{\rm cell}(t) d^3]$. We assume the van der Waals coefficient [22] $\alpha = 1900\,{\rm K\AA}^3$ and use the measured $T_{\rm cell}(t)$ shown in the inset of fig. 3(a). Because of this desorption the film thins at a rate $\dot{d} = d_0(-\dot{n}_{\rm d} V + \dot{n}_{\rm a} V)/N_0$, where the first term in the parentheses is the rate of desorption from the film and the second term is the rate of adsorption from the ^{3}He vapor back into the film. Here N_0 is the number of ^{3}He atoms per monolayer, d_0 is the thickness of

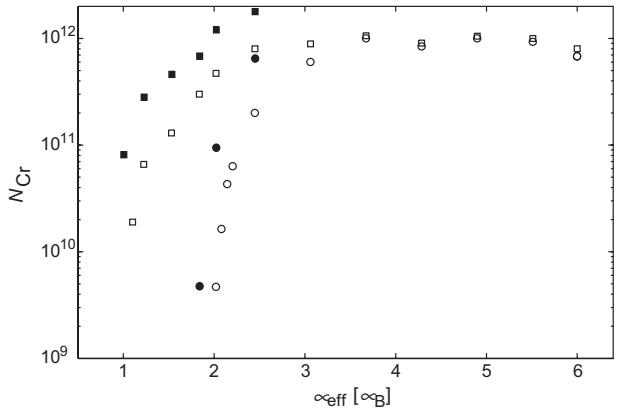

Fig. 4 – Trapping as a function of $\mu_{\rm eff}$. Open symbols show data for $T_{\rm cell} = 550\,{\rm mK}$, closed symbols for $T_{\rm cell} = 470\,{\rm mK}$. These values refer to the temperature of the cell just before the ablation. Squares: number of atoms trapped 300 ms after the valve opens. Circles: number of atoms trapped and thermally isolated 10 s after the valve opens. Slight variations in $T_{\rm cell}$ give rise to $\sim 10\%$ fluctuations in the data.

a monolayer and $\dot{n}_{\rm a} = n_{\rm He} f \frac{A}{V} \sqrt{\frac{k_{\rm B}T}{2\pi m}}$. Finally, the rate of change of the ^{3}He density in the cell is the difference between the outflux of atoms (to the cryopump) and the net influx of atoms (off the cell walls): $\dot{n}_{\rm He} = -\frac{n_{\rm He}}{\tau_{\rm pump}} - \dot{n}_{\rm a} + \dot{n}_{\rm d}$. We solve this series of equations numerically for $d(t)$, $\dot{n}_{\rm d}(t)$, $\dot{n}_{\rm a}(t)$ and $n_{\rm He}(t)$.

The results of this model are shown in fig. 3(b), and account qualitatively for the data. At first, $n_{\rm He}$ rapidly drops three orders of magnitude (as $e^{-t/\tau_{\rm pump}}$) but then slows due to the desorbing film [23]. This slowing prolongs the thermal contact between the Cr and the cell, and for small $\mu_{\rm eff}$ gives rise to the loss seen in fig. 3(a). The shut-off of this loss after 5 s is consistent with the simulations in ref. [11] which show that loss due to thermal contact with the cell walls decreases rapidly for $n_{\rm He} < 10^{13}\,{\rm cm}^{-3}$.

The value of $n_{\rm He}$ calculated at long times ($10^8\,{\rm cm}^{-3}$, inset of fig. 3(b)) is consistent with the lifetime τ_1 observed in the no-bake-out evaporative cooling data of fig. 2(b). Including the "bake-out" routine in the simulation decreases the long-time value of $n_{\rm He}$, consistent with fig. 2(b).

The effect of the film depends strongly upon $T_{\rm cell}(t)$: lower $T_{\rm cell}$ means less energetic ^{3}He-Cr collisions, and a drop in $T_{\rm cell}$ after the valve opens effectively cryopumps the film (lowering $n_{\rm He}$). Calculations of $n_{\rm He}(t)$ for slightly improved base temperature and cooling rate of the cell are shown as dashed lines in figs. 3(a) and (b) and indicate that modest improvements in $T_{\rm cell}(t)$ can result in much faster breaking of thermal contact.

Our results are summarized in fig. 4. The square points show the number of trapped atoms 300 ms after the valve is opened. These atoms have survived the "wind" and the removal of $\sim 99\%$ of the buffer gas (fig. 3(b)), but are still in thermal contact with the cell walls. The number of atoms remaining in the trap 10 s after the valve opens is shown as circles. These atoms are thermally isolated and so can be cooled further by evaporation. The difference between $N_{\rm Cr}$ at 300 ms and 10 s is appreciable only for $\mu_{\rm eff} < 3\mu_{\rm B}$ and is overwhelmingly due to the desorbing film. Small improvements in the thermal performance of the cell can lessen the effect of the film (as described above), and can ensure that atoms trapped at 300 ms remain trapped. Further mitigation of the film can be achieved by coating the cell walls with alkali

metal (*e.g.*, by *in situ* laser ablation). The small binding energy of He on Na or Rb [22] implies that the entire He film should desorb from such a surface on a time scale shorter than τ_{pump}.

For $\mu_{\mathrm{eff}} \geq 3\mu_{\mathrm{B}}$, the number of trapped and thermally isolated atoms is only limited by the ablation yield. 100 times greater yields of thermalized atoms have been produced by ablating less refractory metals such as Na [15].

We have also found that for $\mu_{\mathrm{eff}} = 6\mu_{\mathrm{B}}$, it is possible to trap and thermally isolate atoms with $T_{\mathrm{cell}} > 1.5\,\mathrm{K}$. This allows the study of large-μ atoms using only a pumped ^{4}He cryostat.

In conclusion, we have extended buffer gas trapping to new regimes, allowing the cooling and trapping of a much wider range of atoms and molecules than has previously been possible.

* * *

We acknowledge the assistance of J. Helton, A. Jayich and B. Zygelman. This work was supported by the NSF through the Harvard/MIT Center for Ultracold Atoms.

REFERENCES

[1] Doyle J. M., *Bull. Am. Phys. Soc.*, **39** (1994) 1166; Doyle J. M. *et al.*, *Phys. Rev. A*, **52** (1995) R2515. For buffer gas cooling of charged particles, see Douglas D. J. and French J. B., *J. Am. Soc. Mass Spectrom.*, **3** (1992) 398; Murphy T. J. and Surko C. M., *Phys. Rev. A.*, **46** (1992) 5696.
[2] Wieman C. E. *et al.*, *Rev. Mod. Phys.*, **71** (1999) S253.
[3] Hess H. F. *et al.*, *Phys. Rev. Lett.*, **59** (1987) 672.
[4] Schmidt P. O. *et al.*, *Phys. Rev. Lett.*, **91** (2003) 193201.
[5] Krems R. V. *et al.*, *Phys. Rev. A*, **66** (2002) 30702; Hensler S. *et al.*, quant-ph/0307184.
[6] Goral K. *et al.*, *Phys. Rev. Lett.*, **88** (2002) 170406; Baranov M. A. *et al.*, *Phys. Rev. A*, **66** (2002) 013606; Santos L. *et al.*, *Phys. Rev. Lett.*, **90** (2003) 250403.
[7] Nguyen A. T. *et al.*, physics/0308104.
[8] Ketterle W., *Physica B*, **280** (2000) 11; Shvarchuck I. *et al.*, *Phys. Rev. Lett.*, **89** (2002) 270404.
[9] Kim Jinha *et al.*, *Phys. Rev. Lett.*, **78** (1997) 3665.
[10] Weinstein J. D. *et al.*, *Phys. Rev. A*, **65** (2002) 021604; Hancox C. I. *et al.*, in preparation.
[11] Michniak R. A. *et al.*, in preparation.
[12] Harris J. G. E. *et al.*, *Rev. Sci. Instrum.*, **75** (2004) 17.
[13] Roth A., *Vacuum Technology* (North-Holland, Amsterdam) 1996.
[14] Weinstein J. D., Ph.D. Thesis, Harvard University (2002).
[15] deCarvalho R. *et al.*, in preparation.
[16] Egorov D. *et al.*, *Phys. Rev. A*, **66** (2002) 043401.
[17] We determine n_{He} from the diffusion rate of the Cr atoms without a trapping field.
[18] Ketterle W. and Van Druten N. J., *Adv. At. Mol. Opt. Phys.*, **37** (1996) 181.
[19] Davis K. B. *et al.*, *Phys. Rev. Lett.*, **75** (1995) 3969; Hansel W. *et al.*, *Nature*, **413** (2001) 498.
[20] Sinvani M. *et al.*, *Phys. Rev. Lett.*, **51** (1983) 188.
[21] Roth J. A. *et al.*, *Phys. Rev. Lett.*, **44** (1980) 333.
[22] Vidali G. *et al.*, *Surf. Sci. Rep.*, **12** (1991) 133.
[23] The same calculations give 4.7×10^4 Cr-^{3}He collisions per Cr atom in the 200 s after the valve opens, 98% of which occur in the first 0.5 s.